

Integrating Uncertainty Awareness into Conformalized Quantile Regression

Raphael Rossellini^{*1}, Rina Foygel Barber¹, and Rebecca Willett^{1,2}

¹Department of Statistics, University of Chicago

²Department of Computer Science, University of Chicago

June 16, 2023

Abstract

Conformalized Quantile Regression (CQR) is a recently proposed method for constructing prediction intervals for a response Y given covariates X , without making distributional assumptions. However, as we demonstrate empirically, existing constructions of CQR can be ineffective for problems where the quantile regressors perform better in certain parts of the feature space than others. The reason is that the prediction intervals of CQR do not distinguish between two forms of uncertainty: first, the variability of the conditional distribution of Y given X (i.e., aleatoric uncertainty), and second, our uncertainty in estimating this conditional distribution (i.e., epistemic uncertainty). This can lead to uneven coverage, with intervals that are overly wide (or overly narrow) in regions where epistemic uncertainty is low (or high). To address this, we propose a new variant of the CQR methodology, Uncertainty-Aware CQR (UACQR), that explicitly separates these two sources of uncertainty to adjust quantile regressors differentially across the feature space. Compared to CQR, our methods enjoy the same distribution-free theoretical guarantees for coverage properties, while demonstrating in our experiments stronger conditional coverage in simulated settings and tighter intervals on a range of real-world data sets.

1 Introduction

While machine learning approaches in recent years have frequently succeeded in producing models that produce predictions with low error on average, there are many instances in which these models can provide a false sense of precision. Prediction intervals are one of the most natural ways to quantify uncertainty, providing bounds on the true response that hold with some desired probability, frequently 90%. To this end, conformal prediction

^{*}raphaelr@uchicago.edu

has emerged as an attractive paradigm for creating statistically-valid prediction intervals for black-box machine learning models with no distributional assumptions. Specifically, suppose we have observed n samples $(X_i, Y_i) \in \mathbb{R}^P \times \mathbb{R}$, and we desire a prediction interval for Y_{n+1} based on X_{n+1} . If the $n + 1$ samples are exchangeable (e.g., if the pairs (X_i, Y_i) are drawn i.i.d. from an arbitrary shared distribution), conformal prediction allows one to construct an interval $\hat{C}_n(X_{n+1})$ such that

$$\mathbb{P} \left\{ Y_{n+1} \in \hat{C}_n(X_{n+1}) \right\} \geq 1 - \alpha \quad (1)$$

A remaining challenge is the ability to provide prediction intervals that hold conditionally on the test point's covariates,

$$\mathbb{P} \left\{ Y_{n+1} \in \hat{C}_n(X_{n+1}) \mid X_{n+1} = x \right\} \geq 1 - \alpha,$$

which is not ensured by conformal prediction under the exchangeability assumption alone. Unfortunately, it is impossible for any distribution-free approach to guarantee conditional coverage in a non-trivial way when the covariates follow a continuous distribution [27, 18, 2].

In spite of this impossibility result, there have been numerous methodological advances that allow conformal prediction to provide better conditional coverage properties empirically. A particularly notable advancement has been Conformalized Quantile Regression (CQR) [23], which uses quantile regressors as inputs into the conformal prediction paradigm to create prediction intervals that adapt to the covariates. Part of the appeal is that the true conditional quantile functions are a sufficient ingredient to achieving conditional coverage. If we let $q_{Y|X}(x; \alpha_{\text{lo}})$, $q_{Y|X}(x; \alpha_{\text{hi}})$ be the $\alpha_{\text{lo}}, \alpha_{\text{hi}}$ conditional quantiles for $Y \mid X = x$, where $\alpha_{\text{lo}} = \alpha/2$ and $\alpha_{\text{hi}} = 1 - \alpha/2$, then by construction

$$\mathbb{P} \left\{ Y \in [q_{Y|X}(X; \alpha_{\text{lo}}), q_{Y|X}(X; \alpha_{\text{hi}})] \mid X = x \right\} \geq 1 - \alpha.$$

Thus, if one can find accurate quantile regressors via machine learning, CQR holds potential to create prediction intervals that approximately have conditional coverage while maintaining the marginal validity of previous conformal prediction methods. Specifically, for any $a \in (0, 1)$, let $\hat{q}_{Y|X}(x, a)$ denote an estimate of the conditional a -quantile of $Y \mid X = x$ computed using training data. CQR generates prediction intervals of the form

$$\hat{C}_n(X_{n+1}) = [\hat{q}_{Y|X}(X_{n+1}; \alpha_{\text{lo}}) - t, \hat{q}_{Y|X}(X_{n+1}; \alpha_{\text{hi}}) + t],$$

where calibration data is selected to choose t .

In practice, however, quantile regression is difficult, and our estimate $\hat{q}_{Y|X}(x, a)$ may be less accurate in particularly challenging regions of the feature space. CQR struggles in this setting since it simply inflates the initial estimates by a constant, non-adaptive additive adjustment $t \in \mathbb{R}$.

Others have implemented adaptive variants. For example, the CQR-r variant from Sesia and Candès [25] multiplies t by the interval width $w(x) = \hat{q}_{Y|X}(x; \alpha_{\text{hi}}) - \hat{q}_{Y|X}(x; \alpha_{\text{lo}})$, which yields:

$$\hat{C}_n(X_{n+1}) = [\hat{q}_{Y|X}(X_{n+1}; \alpha_{\text{lo}}) - t \cdot w(X_{n+1}), \hat{q}_{Y|X}(X_{n+1}; \alpha_{\text{hi}}) + t \cdot w(X_{n+1})]$$

The issue here is that this is scaling t by the wrong type of uncertainty. $w(x)$ is a proxy for *aleatoric uncertainty*—the irreducible uncertainty inherent to a data generating process, i.e., the amount of variability in the conditional distribution of $Y | X$. However, the gap between the upper and lower quantile regressors already accounts for aleatoric uncertainty. The additive adjustment should ideally scale with the *epistemic uncertainty*—the scale of the estimation error of the quantile regressors at each X . The aleatoric uncertainty may be associated with epistemic uncertainty in many contexts, but there is no guarantee that there must be a correspondence between the two. In medical studies, for instance, a poorly-represented demographic could have a narrower range of outcomes on average than a well-represented one, meaning that this subpopulation has high epistemic uncertainty yet low aleatoric uncertainty. Our work centers on the idea that, for this type of setting, the quantile-based prediction interval should be calibrated (i.e., inflated) in a way that scales with how well sampled each demographic is (epistemic uncertainty), rather than with the estimated range of outcomes for each demographic (aleatoric uncertainty).

1.1 Our contribution

We propose a new family of methods for conformalizing quantile regression that incorporate epistemic uncertainty. We call them *UACQR-S* (*Uncertainty-Aware CQR via Scaling*) and *UACQR-P* (*Uncertainty-Aware CQR via Percentiles*)¹ UACQR-S creates prediction intervals of a similar form to CQR-r, but its scaling function directly estimates the epistemic, rather than aleatoric, uncertainty in $Y | X$ at each value of X . In contrast, UACQR-P is constructed based on an ensemble of quantile regression estimates (e.g., obtained via bootstrapping the training sample), and outputs a prediction interval that is defined as a calibrated percentile of the B different estimates at each point. Our methods offer the same distribution-free guarantee of validity as existing CQR constructions, while offering empirical improvements in terms of conditional coverage and precision (i.e., interval width).

To minimize computational concerns, we provide recipes for implementing UACQR-S and UACQR-P that have the same computational cost of CQR when using any one of a broad range of machine learning paradigms, namely (1) bagging (which includes Random Forests) or (2) epoch-based optimization (e.g., neural networks). Undoubtedly these two classes cover a large proportion of successful modern machine learning architectures, so our proposed methods hold potential for widespread applications.

2 Existing methods

In this section, we review split conformal prediction [27] in more depth, and define a generic meta-algorithm that captures all existing variants of CQR.

Suppose we are given a data set $(X_1, Y_1), \dots, (X_n, Y_n)$ and a new test point X_{n+1} for which we would like to predict the response, Y_{n+1} . We limit ourselves to assuming only that $(X_1, Y_1), \dots, (X_{n+1}, Y_{n+1})$ are exchangeable. In its most basic version, split conformal prediction operates as follows. We split the n data points into a training set

¹We provide code implementing UACQR at <https://github.com/rrross/UACQR>

and calibration set of sizes $n_0 + n_1 = n$. After fitting a predictive model $\hat{\mu}$ to the training set $\{(X_i, Y_i) : i = 1, \dots, n_0\}$, we then define

$$\hat{C}_n(X_{n+1}) = \hat{\mu}(X_{n+1}) \pm \hat{t}, \quad (2)$$

where \hat{t} is the $\lceil (1 - \alpha)(n_1 + 1) \rceil$ -th smallest element of the calibration set residuals $\{|Y_i - \hat{\mu}(X_i)| : i = n_0 + 1, \dots, n\}$.

Split conformal prediction is much more general than this simple construction, however, and in particular it can be used to produce prediction intervals of any “shape” rather than restricting ourselves only to constant-width type intervals of the form $\hat{\mu}(x) \pm (\text{constant})$. Gupta et al. [11] describe a formulation based on nested sets: suppose that, given the training data $\{(X_i, Y_i) : i = 1, \dots, n_0\}$, we construct a family of nested prediction bands $\hat{C}_{n_0, t}$ (where $\hat{C}_{n_0, t}(x) \subseteq \mathbb{R}$ is a prediction set or prediction interval at each x), indexed over some set $t \in \mathcal{T} \subseteq \mathbb{R}$. This family is required to be nested, with $\hat{C}_{n_0, t}(x) \subseteq \hat{C}_{n_0, t'}(x)$ for $t < t'$, and also that $\inf_{t \in \mathcal{T}} \hat{C}_{n_0, t}(x) = \emptyset$ and $\sup_{t \in \mathcal{T}} \hat{C}_{n_0, t}(x) = \mathbb{R}$. Then, using the calibration set, define

$$\hat{t} = \inf \left\{ t : \sum_{i=n_0+1}^n \mathbf{1}_{Y_i \in \hat{C}_{n_0, t}(X_i)} \geq (1 - \alpha)(n_1 + 1) \right\}, \quad (3)$$

and return the prediction set $\hat{C}_n(X_{n+1}) := \hat{C}_{n_0, \hat{t}}(X_{n+1})$. To summarize, the training points ($i = 1, \dots, n_0$) define a nested family of prediction bands $\{\hat{C}_{n_0, t}\}$, and then the calibration set ($i = n_0 + 1, \dots, n_1$) is used to choose a particular \hat{t} that selects one prediction band from this family to then provide at least $1 - \alpha$ coverage of the final prediction interval. Vovk et al. [27] and Gupta et al. [11] show any construction of this form offers the distribution-free prediction guarantee (1). To see how this general formulation applies to the simple construction (2) given above, we can simply take $\hat{C}_t(x) = \hat{\mu}(x) \pm t$ for $t \in \mathcal{T} = \mathbb{R}$ to recover the prediction set given in (2).

To relate this construction to the problem of quantile regression, we change the notation to provide prediction sets that are specifically designed to be intervals. Let $\hat{q}_{\text{lo}}(X, t)$ and $\hat{q}_{\text{hi}}(X, t)$ be quantile regressors for $Y | X$, fitted using the training data $\{(X_i, Y_i) : i = 1, \dots, n_0\}$, where $t \mapsto \hat{q}_{\text{lo}}(x, t)$ is decreasing, while $t \mapsto \hat{q}_{\text{hi}}(x, t)$ is increasing. We consider the nested family of sets given by $\hat{C}_{n_0, t}(x) = [\hat{q}_{\text{lo}}(x, t), \hat{q}_{\text{hi}}(x, t)]$, and consequently, split conformal prediction returns the interval

$$\hat{C}_n(X_{n+1}) = \hat{C}_{n_0, \hat{t}}(X_{n+1}) = [\hat{q}_{\text{lo}}(X_{n+1}, \hat{t}), \hat{q}_{\text{hi}}(X_{n+1}, \hat{t})] \quad (4)$$

where, for this specific construction, the definition (3) of \hat{t} simplifies to

$$\hat{t} = \inf \left\{ t : \sum_{i=n_0+1}^n \mathbf{1}_{\hat{q}_{\text{lo}}(X_i, t) \leq Y_i \leq \hat{q}_{\text{hi}}(X_i, t)} \geq (1 - \alpha)(n_1 + 1) \right\}. \quad (5)$$

(To satisfy the conditions outlined above, we also assume that $\inf_{t \in \mathcal{T}} \hat{q}_{\text{lo}}(x, t) = -\infty$ and $\sup_{t \in \mathcal{T}} \hat{q}_{\text{lo}}(x, t) = +\infty$, and $\inf_{t \in \mathcal{T}} \hat{q}_{\text{hi}}(x, t) = -\infty$ and $\sup_{t \in \mathcal{T}} \hat{q}_{\text{hi}}(x, t) = +\infty$.)

Next we review CQR and several related existing methods. Our presentation reformulates each method using the general notation we have just defined.

Conformalized Quantile Regression (CQR) For any $a \in (0, 1)$, let $\hat{q}_{Y|X}(x, a)$ denote an estimate (fitted on the training data set) of the conditional a -quantile of Y given $X = x$. Romano et al. [23] proposed fitting quantile regressors for preset upper and lower quantiles, α_{lo} and α_{hi} (e.g., $\alpha_{\text{lo}} = \alpha/2$ and $\alpha_{\text{hi}} = 1 - \alpha/2$), and then using conformal prediction to select a constant additive adjustment to expand or contract these intervals to ensure marginal coverage. This produces a prediction interval of the form

$$\hat{C}_n(X_{n+1}) = [\hat{q}_{Y|X}(X_{n+1}, \alpha_{\text{lo}}) - \hat{t}, \hat{q}_{Y|X}(X_{n+1}, \alpha_{\text{hi}}) + \hat{t}].$$

By defining

$$\hat{q}_{\text{lo}}(x, t) = \hat{q}_{Y|X}(x, \alpha_{\text{lo}}) - t, \quad \hat{q}_{\text{hi}}(x, t) = \hat{q}_{Y|X}(x, \alpha_{\text{hi}}) + t,$$

indexed by $t \in \mathbb{R}$, we can see that the CQR interval is equal to the general construction (4) above.

CQR-r and CQR-m Sesia and Candès [25] propose a variant to CQR, which they call CQR-r. The prediction interval is given by

$$\begin{aligned} \hat{C}_n(X_{n+1}) = & [\hat{q}_{Y|X}(X_{n+1}, \alpha_{\text{lo}}) - \hat{t} \cdot (\hat{q}_{Y|X}(X_{n+1}, \alpha_{\text{hi}}) - \hat{q}_{Y|X}(X_{n+1}, \alpha_{\text{lo}})), \\ & \hat{q}_{Y|X}(X_{n+1}, \alpha_{\text{hi}}) + \hat{t} \cdot (\hat{q}_{Y|X}(X_{n+1}, \alpha_{\text{hi}}) - \hat{q}_{Y|X}(X_{n+1}, \alpha_{\text{lo}}))], \end{aligned}$$

which we can interpret as scaling the inflation of the interval by the *aleatoric* uncertainty in $Y | X$. This method corresponds to the general construction (4) above obtained with the definitions

$$\begin{aligned} \hat{q}_{\text{lo}}(x, t) &= \hat{q}_{Y|X}(x, \alpha_{\text{lo}}) - t \cdot (\hat{q}_{Y|X}(x, \alpha_{\text{hi}}) - \hat{q}_{Y|X}(x, \alpha_{\text{lo}})), \\ \hat{q}_{\text{hi}}(x, t) &= \hat{q}_{Y|X}(x, \alpha_{\text{hi}}) + t \cdot (\hat{q}_{Y|X}(x, \alpha_{\text{hi}}) - \hat{q}_{Y|X}(x, \alpha_{\text{lo}})), \end{aligned}$$

where $t \in \mathbb{R}$. Sesia and Candès [25]’s CQR-r construction is a variant of the method proposed by Kivaranovic et al. [16] (called “CQR-m” by Sesia and Candès [25]), where the scaling factor instead compares the (estimated) upper and lower quantiles to the (estimated) median:

$$\begin{aligned} \hat{q}_{\text{lo}}(x, t) &= \hat{q}_{Y|X}(x, \alpha_{\text{lo}}) - t \cdot (\hat{q}_{Y|X}(x, 0.5) - \hat{q}_{Y|X}(x, \alpha_{\text{lo}})), \\ \hat{q}_{\text{hi}}(x, t) &= \hat{q}_{Y|X}(x, \alpha_{\text{hi}}) + t \cdot (\hat{q}_{Y|X}(x, \alpha_{\text{hi}}) - \hat{q}_{Y|X}(x, 0.5)), \end{aligned}$$

again with $t \in \mathbb{R}$, leading to the prediction interval

$$\begin{aligned} \hat{C}_n(X_{n+1}) = & [\hat{q}_{Y|X}(X_{n+1}, \alpha_{\text{lo}}) - \hat{t} \cdot (\hat{q}_{Y|X}(X_{n+1}, 0.5) - \hat{q}_{Y|X}(X_{n+1}, \alpha_{\text{lo}})), \\ & \hat{q}_{Y|X}(X_{n+1}, \alpha_{\text{hi}}) + \hat{t} \cdot (\hat{q}_{Y|X}(X_{n+1}, \alpha_{\text{hi}}) - \hat{q}_{Y|X}(X_{n+1}, 0.5))]. \end{aligned}$$

Distributional Conformal Prediction (DCP) An alternative style of approach is proposed by Chernozhukov et al. [5], which uses conformal prediction to select the target upper and lower quantiles for quantile regression to achieve the desired coverage. After

fitting the conditional t -quantile $\hat{q}_{Y|X}(x, t)$ for *every* value $t \in [0, 1]$, the prediction set is given by

$$\hat{C}_n(X_{n+1}) = [\hat{q}_{Y|X}(X_{n+1}, \hat{t}), \hat{q}_{Y|X}(X_{n+1}, 1 - \hat{t})],$$

which corresponds to the general construction (4) above by defining

$$\hat{q}_{\text{lo}}(x, t) = \hat{q}_{Y|X}(x, t), \quad \hat{q}_{\text{hi}}(x, t) = \hat{q}_{Y|X}(x, 1 - t),$$

indexed by $t \in [0, 1]$.

2.1 Limitations of existing methods

To understand the motivation behind our new methods, we briefly consider the limitations of this existing range of constructions. Consider the “baseline” prediction interval $\hat{C}_{\text{base}}(x) = [\hat{q}_{Y|X}(x, \alpha/2), \hat{q}_{Y|X}(x, 1 - \alpha/2)]$, given by running quantile regression on the training set. In many settings, this interval might be more accurate in regions with larger quantities of training data and/or more smoothly varying quantiles, and less accurate in other regions. If we use a method such as a neural network to compute this baseline, typically the baseline interval undercovers on average over the calibration (and test) data, as demonstrated in Romano et al. [23], for example.

For each of the existing methods summarized above, this initial interval \hat{C}_{base} appears in the nested family of sets: specifically, it is recovered by taking $t = 0$ for CQR, CQR-r, and CQR-m (assuming $\alpha_{\text{lo}} = \alpha/2$ and $\alpha_{\text{hi}} = 1 - \alpha/2$), and by taking $t = \alpha/2$ for DCP. Now, if \hat{C}_{base} undercovers on the calibration set, conformal prediction lead us to choose a larger value of \hat{t} , thus inflating \hat{C}_{base} in order to achieve a marginal coverage guarantee (1).

Let us now consider how this inflation behaves. CQR provides an *equal* amount of inflation of $\hat{C}_{\text{base}}(x)$ for every x , while CQR-r and CQR-m provide a *higher* amount of inflation of $\hat{C}_{\text{base}}(x)$ at values x with higher aleatoric uncertainty (i.e., higher variability in the conditional distribution of $Y | X$), and generally this is the case for DCP as well.

In contrast, it would be more efficient to inflate $\hat{C}_{\text{base}}(x)$ primarily at those values x where the initial estimate undercovers—that is, regions with high error in $\hat{q}_{Y|X}(x, a)$ as an estimate of the true conditional a -quantile for $a = \alpha/2$ and/or $a = 1 - \alpha/2$. In other words, we would do best to inflate $\hat{C}_{\text{base}}(x)$ more in regions of high *epistemic* uncertainty, which we define as reducible uncertainty (e.g., uncertainty that could have been reduced if we had more data), following the definitions in Senge et al. [24] and Hüllermeier and Waegeman [12].

Interestingly, the main empirical conclusion of Sesia and Candès [25] is that CQR-r (and the related CQR-m method of Kivaranovic et al. [16]), which provide varying amounts of inflation at different values x , were unable to provide smaller intervals on average than CQR, whose construction has constant inflation at each x . We might be tempted to conclude from this that incorporating local adaptivity into the inflation of CQR is not beneficial. However, in light of our own results, we believe that the issue lies in the fact that CQR-r and CQR-m inflate the baseline interval proportional to the aleatoric uncertainty, which may be completely different from the epistemic uncertainty; thus, we instead conjecture that it is important to be locally adaptive to the right source of uncertainty (that is, epistemic rather than aleatoric).

3 Uncertainty-aware CQR

Our proposal is to integrate uncertainty awareness into CQR via the general construction (4), by explicitly incorporating an estimate of epistemic uncertainty into the construction. We now present two specific proposals that achieve this aim.

UACQR-S Our first proposed method is similar in construction to the approach of CQR-r and CQR-m, where the baseline quantiles are inflated proportional to a scaling factor. (Here the “S” in UACQR-S denotes *scaling*.) We define

$$\hat{q}_{\text{lo}}(x, t) = \hat{q}_{Y|X}(x, \alpha_{\text{lo}}) - t \cdot \hat{g}_{\text{lo}}(x), \quad \hat{q}_{\text{hi}}(x, t) = \hat{q}_{Y|X}(x, \alpha_{\text{hi}}) + t \cdot \hat{g}_{\text{hi}}(x),$$

indexed by $t \in \mathbb{R}$, where $\hat{q}_{Y|X}(x, \alpha_{\text{lo}})$ (respectively, $\hat{q}_{Y|X}(x, \alpha_{\text{hi}})$) is some baseline initial estimator of the conditional α_{lo} - (respectively, α_{hi} -) quantile, while $\hat{g}_{\text{lo}}(x)$ (respectively, $\hat{g}_{\text{hi}}(x)$) estimates the standard deviation of this quantile estimate. (To give a concrete example, if we construct $\hat{q}_{Y|X}^b(x, a)$ ’s via bootstrapping subsamples of the training data for each $a = \alpha_{\text{lo}}, \alpha_{\text{hi}}$, then $\hat{q}_{Y|X}(x, a)$ might be obtained by averaging the B bootstrapped estimates, while $\hat{g}_{\text{lo}}(x)$ and $\hat{g}_{\text{hi}}(x)$ might be computed via the sample standard deviations of the $\hat{q}_{Y|X}^b(x, a)$ ’s at each value of x .)

Applying our general construction (4) then yields the prediction interval

$$\hat{C}_n(X_{n+1}) = [\hat{q}_{Y|X}(X_{n+1}, \alpha_{\text{lo}}) - \hat{t} \cdot \hat{g}_{\text{lo}}(X_{n+1}), \hat{q}_{Y|X}^{(\hat{t})}(X_{n+1}, \alpha_{\text{hi}}) + \hat{t} \cdot \hat{g}_{\text{hi}}(X_{n+1})], \quad (6)$$

where \hat{t} is computed as in (5).

Examining this construction for UACQR-S, we can observe that CQR-r and CQR-m can be written in the same format—for example, by taking $\hat{g}_{\text{lo}}(x) = \hat{q}_{Y|X}(x, 0.5) - \hat{q}_{Y|X}(x, \alpha_{\text{lo}})$ for CQR-m. However, for CQR-r and CQR-m the corresponding scaling factors \hat{g}_{lo} and \hat{g}_{hi} correspond to the aleatoric uncertainty in our initial quantile regression, while our particular choice of the scaling factors \hat{g}_{lo} and \hat{g}_{hi} is aimed at estimating the epistemic uncertainty, thus providing a more useful local adaptivity when inflating the prediction interval.

UACQR-P Our second variant is UACQR-P, where the “P” denotes *percentile*. To begin, we compute an ensemble of B estimates of $q_{Y|X}(x, \alpha_{\text{lo}})$ and of $q_{Y|X}(x, \alpha_{\text{hi}})$, denoted by $\hat{q}_{Y|X}^b(x, a)$ for each $b \in \{1, \dots, B\}$ and each $a \in \{\alpha_{\text{lo}}, \alpha_{\text{hi}}\}$. (For instance, we may obtain these by running a quantile regression procedure on B different samples bootstrapped from the training set.)

Let $\hat{q}_{Y|X}^{(b)}(x, a)$ refer to the b -th order statistic for each $a = \alpha_{\text{lo}}, \alpha_{\text{hi}}$, so that the estimates are now sorted, with $\hat{q}_{Y|X}^{(1)}(x, a) \leq \dots \leq \hat{q}_{Y|X}^{(B)}(x, a)$. We also define $\hat{q}_{Y|X}^{(0)}(x, a) = -\infty$ and $\hat{q}_{Y|X}^{(B+1)}(x, a) = +\infty$. Then defining

$$\hat{q}_{\text{lo}}(x, t) = \hat{q}_{Y|X}^{(B+1-t)}(x, \alpha_{\text{lo}}), \quad \hat{q}_{\text{hi}}(x, t) = \hat{q}_{Y|X}^{(t)}(x, \alpha_{\text{hi}}),$$

over the index set $t \in \mathcal{T} = \{0, 1, \dots, B, B + 1\}$, applying our general construction (4) yields the prediction interval

$$\hat{C}_n(X_{n+1}) = [\hat{q}_{Y|X}^{(B+1-\hat{t})}(X_{n+1}, \alpha_{\text{lo}}), \hat{q}_{Y|X}^{(\hat{t})}(X_{n+1}, \alpha_{\text{hi}})], \quad (7)$$

where \hat{t} is computed as in (5).

One useful property of this construction is that it preserves the smoothness properties of the underlying base estimators—in the Appendix D, we show that if each of the bootstrapped estimates $\hat{q}_{Y|X}^b(x, a)$ is Lipschitz as a function of x , then each order statistic $\hat{q}_{Y|X}^{(b)}(x, a)$ is Lipschitz as well.

3.1 Strategies for estimating epistemic uncertainty

In UACQR-P, epistemic uncertainty is estimated indirectly, via producing an ensemble of quantile estimates $\{\hat{q}_{Y|X}^b(x, a)\}_{b=1, \dots, B}$ at each $a = \alpha_{\text{lo}}, \alpha_{\text{hi}}$. For UACQR-S, in contrast, we require explicit estimates of epistemic uncertainty, $\hat{g}_{\text{lo}}(x)$ and $\hat{g}_{\text{hi}}(x)$. Here we outline a few potential strategies for generating these ensembles or these uncertainty estimates.

- **Bootstrapping/bagging.** We can generate a collection $\{\hat{q}_{Y|X}^b(x, a)\}_{b=1, \dots, B}$ by training each $\hat{q}_{Y|X}^b$ on a different subset of the training data, e.g., by bootstrapping [8] the training set. The empirical distribution of this collection approximates the distribution of $\hat{q}_{Y|X}$ under different draws of the training data. For UACQR-S, we can compute

$$\hat{q}_{Y|X}(x, \alpha_{\text{lo}}) = \frac{1}{B} \sum_{b=1}^B \hat{q}_{Y|X}^b(x, \alpha_{\text{lo}})$$

and

$$\hat{g}_{\text{lo}}(x) = \left[\frac{1}{B-1} \sum_{b=1}^B (\hat{q}_{Y|X}^b(x, \alpha_{\text{lo}}) - \hat{q}_{Y|X}(x, \alpha_{\text{lo}}))^2 \right]^{1/2},$$

and $\hat{q}_{Y|X}(x, \alpha_{\text{hi}})$ and $\hat{g}_{\text{hi}}(x)$ are defined analogously. Of course, we might also choose to use a different aggregation procedure, e.g., a median or quantile of the bootstrapped estimates, rather than the mean, which corresponds to bagging [3]. In Appendix A, we discuss how we may implement our methods efficiently with Quantile Regression Forests [21] even with their unique aggregation procedure.

- **Epochs of training.** Previous work has indicated that neural networks can fit “easy” regions of the feature space well in early epochs while “difficult” regions are not fit until later epochs. For instance, Mangalam and Prabhu [20] show that deep neural networks learn examples which are learnable by shallow networks first, suggesting that the number of epochs until a training sample is accurately learned may reflect its epistemic uncertainty. Therefore, a heuristic for epistemic uncertainty is to measure how much a neural network’s predictions change across epochs. Here, $\{\hat{q}_{Y|X}^b(x, a)\}_{b=1, \dots, B}$ would refer to the model’s predictions after each epoch b . This

heuristic may be more suitable for UACQR-S than UACQR-P, since ensemble members corresponding to later epochs may be higher quality than those of earlier epochs.

- **A parametric approach.** Some quantile regression models may provide a distribution for its estimates under parametric assumptions, such as linear quantile regression [17]. Specifically, for UACQR-S, the quantile estimates $\hat{q}_{Y|X}(x, \alpha_{\text{lo}})$ and $\hat{q}_{Y|X}(x, \alpha_{\text{hi}})$ would be fitted via some parametric model (e.g., linear quantile regression), and the scaling parameters $\hat{g}_{\text{lo}}(x)$ and $\hat{g}_{\text{hi}}(x)$ would then be defined as the standard errors of these quantile estimates, as calculated according to the parametric model.

3.2 Theoretical guarantee

Theorem 1. *Assume the data points $(X_1, Y_1), \dots, (X_n, Y_n), (X_{n+1}, Y_{n+1})$ are exchangeable. Then the UACQR-P and UACQR-S prediction intervals constructed in (7) and (6), respectively, satisfy the marginal coverage guarantee $\mathbb{P}\{Y_{n+1} \in \hat{C}_n(X_{n+1})\} \geq 1 - \alpha$.*

Proof. This result follows immediately from the properties of conformal prediction [27, 11], once we observe that UACQR-P and UACQR-S can be formulated as a special case of the nested conformal prediction construction, as detailed in (4). \square

4 Simulation case study

In this section, we demonstrate our methods on simulated data in which we can highlight the differences between aleatoric and epistemic uncertainty. We generate simulated data from the distribution

$$X \sim \text{Beta}(1.2, 0.8), \quad Y | X \sim N(\sin(X^{-3}), X^2),$$

with sample size $n = 100$ (and dimension $p = 1$). We compare our UACQR-P and UACQR-S methods against the existing CQR and CQR-r methods, and repeat the experiment for 150 independent trials. For all four methods, the base quantile regression method is a neural network—we note that this base estimator exhibits substantial overfitting in this simulation. Details of the implementation of all four methods are given in Appendix B. We set $\alpha = 0.1$ to create 90% prediction intervals.

Results. Figure 1 shows the resulting prediction bands constructed by each of the four methods, for one trial of the experiment. We also show the oracle prediction interval, given by $[q_{Y|X}(x, \alpha/2), q_{Y|X}(x, 1 - \alpha/2)]$ (where these now refer to the *true* conditional quantiles of $Y | X$).

Examining the oracle prediction interval, in each chart, we can see the distinction between aleatoric and epistemic uncertainty. *Aleatoric uncertainty* is high near $X = 1$, since the variance of $Y | X$ is higher and thus the oracle prediction interval is relatively wide, and low near $X = 0$, where the variance of $Y | X$ is low and thus the oracle prediction

interval is extremely narrow. *Epistemic uncertainty*, in contrast, is relatively low near $X = 1$, since we have many data points that allow our neural net to fit the region well, and much higher near $X = 0$, since the Beta distribution for the feature X ensures we have very few training samples in this region, and moreover, in this region, the highly nonsmooth conditional mean function is particularly challenging to estimate.

As a consequence, CQR and CQR-r show prediction intervals that are too narrow near $X = 0$, which is compensated for by the overly large inflations of the intervals near $X = 1$. In contrast, UACQR-P and UACQR-S correctly inflate the prediction intervals more in the high-uncertainty region near $X = 0$, and they do not overly inflate the intervals in the more well-informed region near $X = 1$.

In Figure 2, we show the results of the experiment averaged over 150 independent trials, where the figure displays the average conditional coverage, $\mathbb{P}\left\{Y_{n+1} \in \hat{C}_n(X_{n+1}) \mid X_{n+1} = x\right\}$, as a function of the test feature value $x \in [0, 1]$. While all four methods achieve *marginal* coverage (1), averaged over X_{n+1} (as guaranteed by the theory), we observe very different empirical trends in the conditional coverage. Specifically, CQR and CQR-r are undercovering in the region of high epistemic uncertainty (near $X = 0$), and overcovering in regions of lower epistemic uncertainty (higher values of X). In particular, we can also see that the adaptivity of CQR-r to aleatoric uncertainty is counterproductive here, with unnecessarily wide prediction intervals near $X = 1$.

In contrast, UACQR-P and UACQR-S maintain relatively even coverage across the range of X values. Of course, these prediction intervals do not fit accurately to the highly nonsmooth, high-frequency trends in the conditional mean of $Y \mid X$ near $X = 0$, but the wider prediction intervals in this region of high uncertainty compensate appropriately for our inability to estimate this challenging conditional mean. This ability to provide coverage in the high epistemic uncertainty area (near $X = 0$), does not come at the expense of overly wide intervals in the low epistemic uncertainty region (larger values of X); both of the UACQR methods provide close to 90% coverage for both low and high values of X .

5 Performance on real world data sets

We measure the performance of our proposals and baselines on data sets from Romano et al. [23] and Sesia and Candès [25] in Table 1. Six of the twelve data sets included in these studies had a response of 0 for over 25% of samples. This zero-inflation means that methods such as CQR and CQR-r, which inflate the prediction interval symmetrically at the left and right endpoint, are not as well suited for this data. In order to enable a fair comparison with these existing methods, then, we restrict our attention to the remaining six data sets. We used Quantile Regression Forests for these data sets, since they are all tabular and tree-based methods frequently beat neural networks on tabular data [10]. We note the average performance across 20 runs in Table 1. Unlike in the simulation setting, we cannot measure conditional coverage, so our performance metric will instead be the average interval width on test points. The motivation behind this is that, among methods that all have 90% test coverage, the most desirable approach may be one that provides the narrowest intervals on average. Since we use random train-test splits in these experiments,

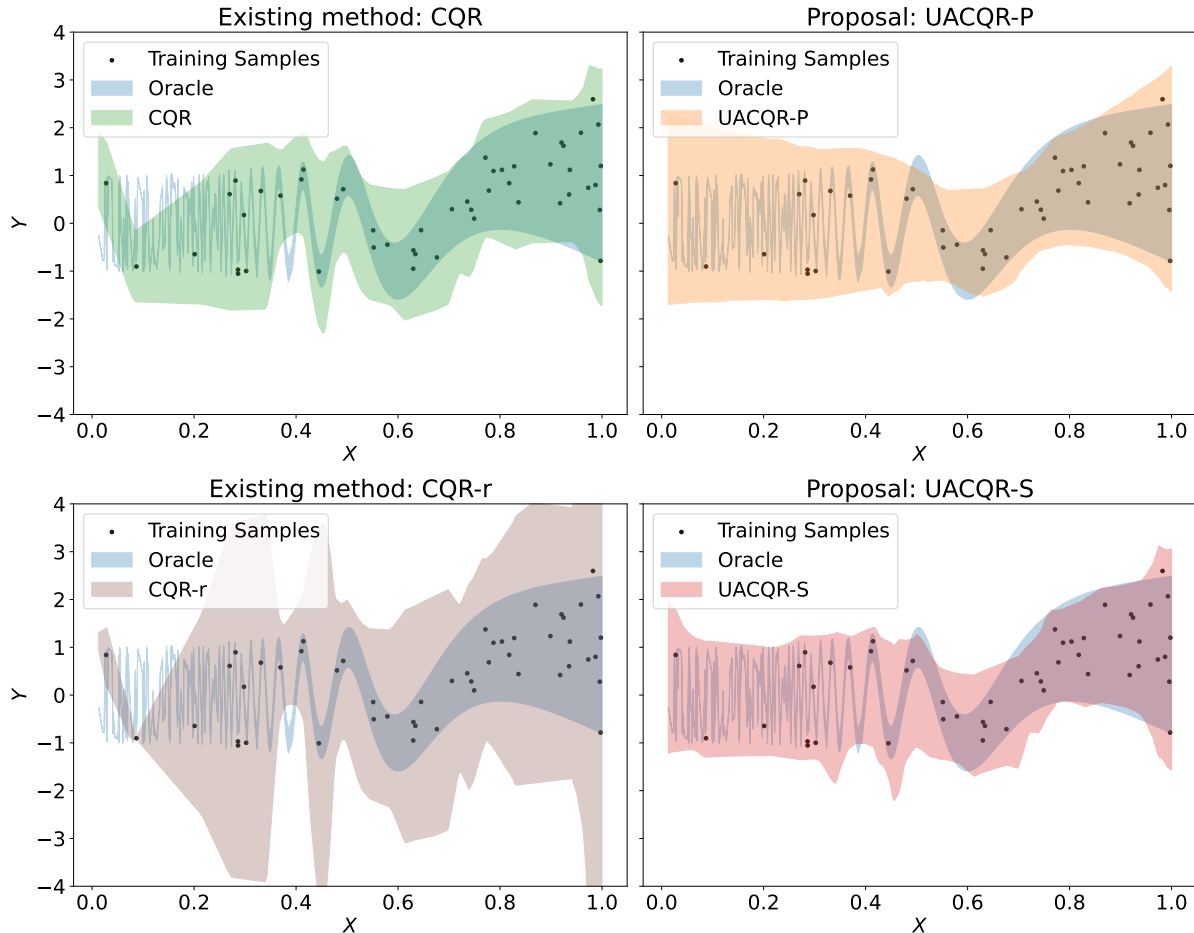


Figure 1: A comparison of the prediction intervals for existing and proposed methods under one random draw from the data generating process. While existing methods will have low conditional coverage in the high epistemic uncertainty region near $X = 0$, our proposals adapt to the toughness of this region. Each conformal procedure is run on the same fitted neural net. For UACQR we use the epoch-based heuristic for epistemic uncertainty. We limit the y-axis to $[-4, 4]$ for visual clarity.

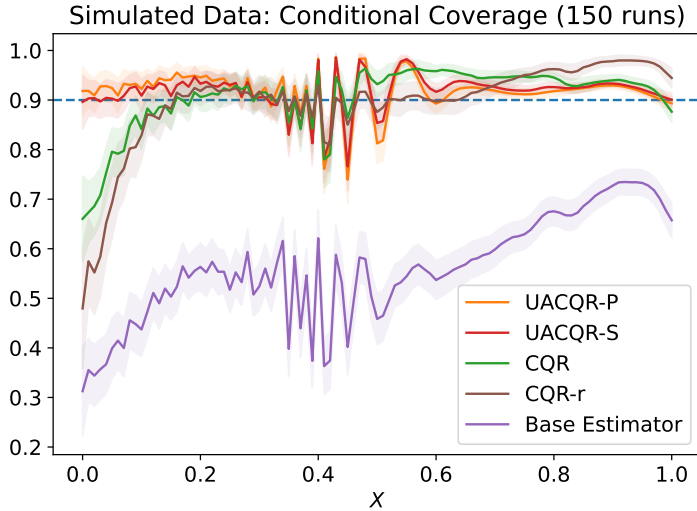


Figure 2: A comparison of the conditional coverage of existing and proposed methods across 150 random draws, with same setting as Figure 1. All existing methods severely undercover near $X = 0$, where epistemic uncertainty is high, while our proposals maintain conditional coverage even in this challenging region.

we ensure exchangeability of the data, and therefore all methods will have above 90% coverage on average. Moreover, we use a randomized conformal procedure, detailed in Appendix C, that ensures all methods average 90% coverage almost exactly. Our choice of hyperparameter (`min_samples_leaf`) for each method was the value that minimized the final average test interval width: usually 5 for UACQR-P and 1 for the rest.

In general, it is not necessarily surprising that UACQR-P frequently outperforms UACQR-S here: like the percentile method in bootstrapping [7], UACQR-P is better equipped to negotiate any skewness in the empirical distribution of $\{\hat{q}_{Y|X}^b(x, a)\}_{b=1, \dots, B}$. In addition, UACQR-P is invariant to monotonically increasing transformations of the response since it is a function of ranks, while UACQR-S is not. Therefore, it is possible that the relative performance of UACQR-S could improve under certain transformations.

6 Discussion and limitations

In this work, we have shown that locally adaptive calibration can be beneficial for conformalizing a quantile regression method, as long as the local adaptivity is capturing the correct information—epistemic, rather than aleatoric, uncertainty, or in other words, the variability of the quantile regression estimates, rather than the variability of the response Y itself.

While our methods have demonstrated strong empirical performance on simulations and real-world data sets alike, there are a few caveats and limitations. First, the performance of our methods is gated by the ability to estimate epistemic uncertainty well. Thus, for bootstrapping and heuristic approaches alike, our methods may be sensitive to the sample

Table 1: Real-world data set results on 20 runs

Dataset	Average Test Interval Width (Standard Error)			
	UACQR-P	UACQR-S	CQR	CQR-r
bike [6, 9]	1.143 (0.009)	1.452 (0.008)	1.481 (0.008)	1.435 (0.008)
bio [6]	1.535 (0.008)	1.650 (0.006)	1.652 (0.006)	1.649 (0.006)
community [6, 22]	1.494 (0.021)	1.750 (0.017)	1.761 (0.016)	1.757 (0.016)
concrete [6, 28]	0.668 (0.008)	0.729 (0.008)	0.745 (0.007)	0.721 (0.008)
homes [14]	0.626 (0.005)	0.693 (0.005)	0.754 (0.005)	0.707 (0.005)
star [1]	0.175 (0.001)	0.175 (0.001)	0.174 (0.001)	0.175 (0.001)

size n and our ensemble size B —if these are not sufficiently large, or if the data exhibits other challenges, attempting to incorporate local adaptivity may be detrimental if our estimate of local epistemic uncertainty is too noisy. A second potential limitation is that, depending on the specific methods used to compute the initial collection of B estimates, UACQR may present users with a computational-statistical tradeoff.

On the other hand, if epistemic uncertainty is estimated reasonably well, then (as we see in our experiments), UACQR has the potential to offer prediction intervals that are both shorter overall, and better able to achieve conditional coverage that is roughly constant across both easier and harder regions of the feature space. This demonstrates the benefits of a more locally adaptive approach when implementing conformal prediction, and may offer insights for improving the empirical performance of conformal prediction on problems beyond quantile regression, as well.

7 Acknowledgements

R.F.B. was partially supported by the National Science Foundation via grant DMS-2023109, and by the Office of Naval Research via grant N00014-20-1-2337. R.M.W. was partially supported by the National Science Foundation via grants DMS-1930049 and NSF DMS-2023109, and by the Department of Energy via grant DE-AC02-06CH113575.

References

- [1] Achilles, C., Bain, H. P., Bellott, F., Boyd-Zaharias, J., Finn, J., Folger, J., Johnston, J., and Word, E. (2008). Tennessee’s student teacher achievement ratio (STAR) project. Accessed: July, 2019.
- [2] Barber, R. F., Candes, E. J., Ramdas, A., and Tibshirani, R. J. (2021). The limits of distribution-free conditional predictive inference. *Information and Inference: A Journal of the IMA*, 10(2):455–482.
- [3] Breiman, L. (1996). Bagging predictors. *Machine Learning*, 24(2):123–140.

[4] Chernozhukov, V., Fernández-Val, I., and Galichon, A. (2010). Quantile and probability curves without crossing. *Econometrica*, 78(3):1093–1125.

[5] Chernozhukov, V., Wüthrich, K., and Zhu, Y. (2021). Distributional conformal prediction. *Proceedings of the National Academy of Sciences*, 118(48):e2107794118.

[6] Dua, D. and Graff, C. (2017). UCI machine learning repository.

[7] Efron, B. (1981). Nonparametric standard errors and confidence intervals. *canadian Journal of Statistics*, 9(2):139–158.

[8] Efron, B. and Tibshirani, R. J. (1993). *An Introduction to the Bootstrap*. Number 57 in Monographs on Statistics and Applied Probability. Chapman & Hall/CRC, Boca Raton, Florida, USA.

[9] Fanaee-T, H. and Gama, J. (2013). Event labeling combining ensemble detectors and background knowledge. *Progress in Artificial Intelligence*, pages 1–15.

[10] Grinsztajn, L., Oyallon, E., and Varoquaux, G. (2022). Why do tree-based models still outperform deep learning on tabular data? *arXiv preprint arXiv:2207.08815*.

[11] Gupta, C., Kuchibhotla, A. K., and Ramdas, A. (2022). Nested conformal prediction and quantile out-of-bag ensemble methods. *Pattern Recognition*, 127:108496.

[12] Hüllermeier, E. and Waegeman, W. (2021). Aleatoric and epistemic uncertainty in machine learning: An introduction to concepts and methods. *Machine Learning*, 110:457–506.

[13] Ioffe, S. and Szegedy, C. (2015). Batch normalization: Accelerating deep network training by reducing internal covariate shift. In *International conference on machine learning*, pages 448–456. pmlr.

[14] Kaggle (2016). House sales in King County, USA. <https://www.kaggle.com/harlfoxem/housesalesprediction/metadata>. Accessed: August, 2019.

[15] Kingma, D. P. and Ba, J. (2014). Adam: A method for stochastic optimization. *arXiv preprint arXiv:1412.6980*.

[16] Kivaranovic, D., Johnson, K. D., and Leeb, H. (2020). Adaptive, distribution-free prediction intervals for deep networks. In *International Conference on Artificial Intelligence and Statistics*, pages 4346–4356. PMLR.

[17] Koenker, R. (1994). Confidence intervals for regression quantiles. In Mandl, P. and Hušková, M., editors, *Asymptotic Statistics*, pages 349–359, Heidelberg. Physica-Verlag HD.

- [18] Lei, J. and Wasserman, L. (2014). Distribution-free prediction bands for nonparametric regression. *Journal of the Royal Statistical Society: Series B: Statistical Methodology*, pages 71–96.
- [19] Mammen, E. (1991). Nonparametric regression under qualitative smoothness assumptions. *The Annals of Statistics*, 19(2):741–759.
- [20] Mangalam, K. and Prabhu, V. U. (2019). Do deep neural networks learn shallow learnable examples first? In *ICML 2019 Workshop on Identifying and Understanding Deep Learning Phenomena*.
- [21] Meinshausen, N. (2006). Quantile regression forests. *Journal of Machine Learning Research*, 7(35):983–999.
- [22] Redmond, M. and Baveja, A. (2002). A data-driven software tool for enabling cooperative information sharing among police departments. *European Journal of Operational Research*, 141(3):660–678.
- [23] Romano, Y., Patterson, E., and Candès, E. J. (2019). Conformalized quantile regression. In *NeurIPS*.
- [24] Senge, R., Bösner, S., Dembczyński, K., Haasenritter, J., Hirsch, O., Donner-Banzhoff, N., and Hüllermeier, E. (2014). Reliable classification: Learning classifiers that distinguish aleatoric and epistemic uncertainty. *Information Sciences*, 255:16–29.
- [25] Sesia, M. and Candès, E. J. (2020). A comparison of some conformal quantile regression methods. *Stat*, 9(1):e261.
- [26] Srivastava, N., Hinton, G., Krizhevsky, A., Sutskever, I., and Salakhutdinov, R. (2014). Dropout: a simple way to prevent neural networks from overfitting. *The journal of machine learning research*, 15(1):1929–1958.
- [27] Vovk, V., Gammerman, A., and Shafer, G. (2005). *Algorithmic Learning in a Random World*. Springer-Verlag, Berlin, Heidelberg.
- [28] Yeh, I.-C. (1998). Modeling of strength of high-performance concrete using artificial neural networks. *Cement and Concrete research*, 28(12):1797–1808.

A Fast heuristic alternatives to bootstrapping

We propose several ways to implement UACQR-P and UACQR-S without needing to refit the base learned model B times.

A.1 Quantile Regression Forests

We first describe what happens when one runs Quantile Regression Forests (QRF) [21] on a dataset to learn the a -quantile. The model is composed of N decision trees, each trained with a bootstrapped sample of points. To make a prediction, we start by feeding the point’s covariates X_i through each of the decision trees and note which leaves X_i resides in. We then take the weighted a -quantile of the responses of the training samples in these leaves, where the weights correspond to multiplicity of the training samples in this collection. See Figure 3 for reference.

Instead of refitting B full QRFs on bootstrapped training sets, we instead leverage the bootstrapping already done in fitting a single QRF. Namely, we estimate the a -quantile in each leaf that X_i resides in and use these N estimates as an ensemble of estimates. Observe that this is equivalent to running UACQR with $B = N$ on QRF models with only one tree in each model. This entails setting $\{\hat{q}_{Y|X}^b(x, a)\}_{b=1, \dots, B}$ to be the estimate of the a -quantile in each tree.

For UACQR-S, we can use the standard deviation of this set for $\hat{g}_{\text{lo}}(x)$ when $a = \alpha_{\text{lo}}$ and similarly for $\hat{g}_{\text{hi}}(x)$. In our implementations, we set $\hat{q}_{Y|X}(x, a)$ to be the output of the full QRF, with $B = N$ trees, for the a -quantile. The reason is that this allows the base estimator to be QRF as originally designed, with the heuristic only being used for estimating $\hat{g}_{\text{lo}}(x), \hat{g}_{\text{hi}}(x)$.

A.2 Epoch-based Optimization

Previous work has indicated that neural networks can fit “easy” regions of the feature space well in early epochs while “difficult” regions are not fit until later epochs. For instance, Mangalam and Prabhu [20] show that deep neural networks learn examples which are learnable by shallow networks first, suggesting that the number of epochs until a training sample is accurately learned may reflect its epistemic uncertainty.

Using this idea as a heuristic, one way to approximate epistemic uncertainty is to measure how much a neural network’s predictions change across epochs. Here, $\{\hat{q}_{Y|X}^b(x, a)\}_{b=1, \dots, B}$ would refer to the model’s predictions after each epoch b . We can use the standard deviation of this set for $\hat{g}_{\text{lo}}(x)$ when $a = \alpha_{\text{lo}}$ and similarly for $\hat{g}_{\text{hi}}(x)$.

There are two ways to implement this epoch-based heuristic. First, during training, one can store the model’s predictions on the held-out samples after each epoch. This may not be feasible if we receive the data in an online fashion and need to train the quantile regressors without access yet to the calibration and test data. Second, one can copy the neural network’s parameters after each epoch, and then we can later reload each of these copies during calibration and test to see how the model’s predictions for the held-out data

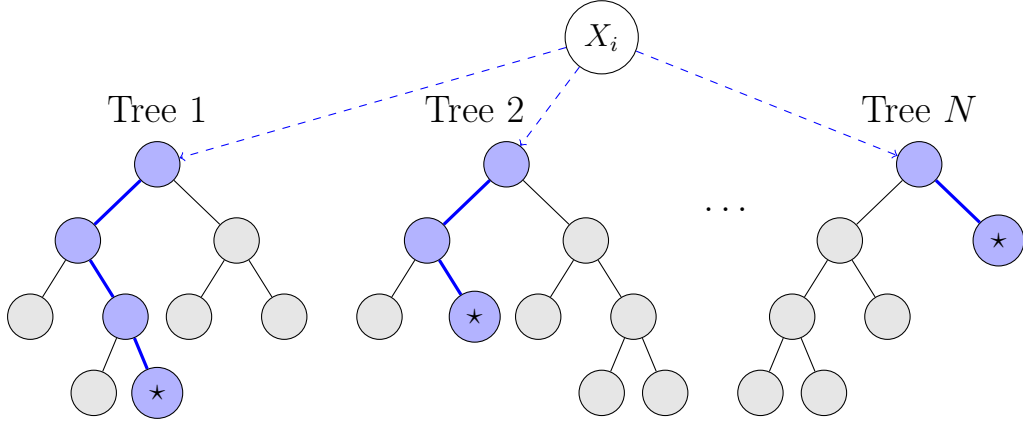


Figure 3: Illustration of a Random Forest, which serves as a visual aid for the ensuing discussion on existing and proposed methods. **QRF** outputs the empirical $\alpha_{\text{lo}}, \alpha_{\text{hi}}$ quantiles of the collection of all responses in all the leaves associated with X_i (marked with a star for each tree). **CQR** then calibrates a constant additive adjustment to these to get $1 - \alpha$ coverage. Our sped-up **UACQR-P** calculates the empirical $\alpha_{\text{lo}}, \alpha_{\text{hi}}$ quantiles in *each* leaf associated with X_i (marked with a star) and then calibrates how to aggregate these quantile estimates to get $1 - \alpha$ coverage.

changed across epochs. This is more memory intensive, however we did not encounter any problems when using this second approach for our experiments.

One wrinkle, though, is that the user may view the model trained for B epochs as the highest quality estimate. In this case, for UACQR-S we may consider letting $\hat{q}_{Y|X}(x, a) = \hat{q}_{Y|X}^B(x, a)$ for $a \in \{\alpha_{\text{lo}}, \alpha_{\text{hi}}\}$, i.e., the lower and upper bounds of our prediction intervals, pre-conformal, are the fully trained models. This is in fact what we do for our experiments.

It is not quite as easy to privilege the fully-trained model with UACQR-P, and therefore this heuristic may be more suitable for UACQR-S. A subject of future research may be to take weighted percentiles of $\{\hat{q}_{Y|X}^b(x, a)\}_{b=1, \dots, B}$ for UACQR-P, where weights increase with b . Alternatively, in the bootstrapping literature there is the bias-corrected percentile method [7] that, in their setting, incorporates an estimator that uses all of the training samples into the confidence interval construction.

B Methodological Details

All of our experiments were done on a computing cluster, with no extra memory allocations or extra computing nodes requested. We use 150 trials for simulations and 20 trials for the real-world data set experiments. In each trial, we have a new draw of the data (training, calibration, and test) and a different random initialization of the model.

B.1 Simulation

We use a neural network with 2 hidden layers, with 100 nodes in each, and ReLU activations for each hidden layer. The neural network outputs three responses, each with the different loss function. The first two are trained with quantile loss, with the target quantiles being 0.05 and 0.95. The third response is trained with squared error loss. We find that adding the squared error loss output dimension, while not theoretically necessary for quantile regression, improves finite sample performance. We use batch normalization [13] and min-max normalization of both the inputs and the responses. The parameters of the neural network are initialized using PyTorch’s default setting. We train the neural network for 1000 epochs with a batch size of 2 and an initial learning rate of 0.001. To make batch normalization more stable in the presence of such a small batch size, we use the running moment estimates after the first epoch, instead of continuing to estimate the moments for each batch. We use a step learning rate scheduler, with a decay rate of 0.999 every 10 epochs, and the Adam optimizer [15]. These hyperparameter choices were made to encourage overfitting, since if the neural network learned the conditional quantiles well then the benefits of any of the conformal methods would be minimal. For implementing both UACQR methods, we use the epoch-based heuristic to avoid refitting and set $B = 999$. For UACQR-S, CQR, and CQR-r, we let the base estimator $\hat{q}_{Y|X}(x, a)$ be the fully trained network $\hat{q}_{Y|X}^B(x, a)$.

Quantile crossing is a phenomenon in which a quantile regressor may predict a lower value for an upper quantile than for a lower quantile. This tends to occur out-of-sample, when extrapolating. A common post-processing mechanism to address quantile crossing is isotonization: when estimating two quantiles, in the event of crossing, set the upper and lower quantile outputs equal to the average of the two [19, 4]. We ran our experiments with and without this post-processing and received nearly identical results. The likelihood of quantile crossing was reduced in our simulation setting, since the distribution of X was bounded.

B.2 Real-world data sets

We use Quantile Regression Forests for quantile regression with these data sets. We use default hyperparameter settings, with the exception of `min_samples_leaf`, i.e. the minimum number of samples a leaf can contain. As discussed in Appendix A, the way in which we use Quantile Regression forests is different for UACQR-P from the rest. Since with UACQR-P we calculate the target quantiles in each leaf, there is a heightened need for `min_samples_leaf` to be greater than 1 for our implementation of UACQR-P to have decent estimations in each leaf. In general, we observed that test interval widths were minimized with `min_samples_leaf` equal to 5 for UACQR-P and with `min_samples_leaf` equal to 1 for the rest of the methods. For both UACQR methods, we use $B = 100$. For UACQR-S, CQR, and CQR-r, we let the base estimator $\hat{q}_{Y|X}(x, a)$ be the full QRF, with $B = N = 100$ trees, using the standard QRF implementation.

To ensure exchangeability, we sample the training, calibration, and test sets without replacement from the full data sets. We use 40% of the points for training, 40% for

calibration, and 20% for testing. For computability, for the `bio` and `homes` data sets, we use only use 25% and 50%, respectively, of the full data sets in any run. For clarity, with `bio` in each run 10% of all data points are used for training, 10% for calibration, 5% for testing, and 75% not at all.

As done in Romano et al. [23], we divide the responses by the mean absolute value response of the training set. This ensures that the rows in Table 1 each have similar magnitude.

We do not need to worry about quantile crossing for these experiments, since it is impossible for Quantile Regression Forests: each quantile estimate corresponds to the sample quantile of the same set of samples.

In all experiments, including the additional ones in Appendix E.2, for UACQR-S we calculate $\hat{g}_{\text{lo}}(x), \hat{g}_{\text{hi}}(x)$ using standard deviations, as described in Section 3.1. However, we have observed that UACQR-S’s performance on these real data experiments often improves if we use interquartile range instead, likely due to the metric’s robustness to outliers.

C Randomized cutoffs for exact coverage

The coverage guarantee obtained by methods within the conformal prediction framework is generally written as a lower bound, i.e., $\mathbb{P}\{Y_{n+1} \in \hat{C}_n(X_{n+1})\} \geq 1 - \alpha$. Examining the construction for the nested split conformal case specifically, given in (3) and (4), we can see that the true probability of coverage might be higher than $1 - \alpha$, for two reasons: first, due to rounding error (if $(1 - \alpha)(n_1 + 1)$ is not an integer), and second, due to ties among the conformity scores, which in this case are given by the values

$$t_i = \inf\{t \in \mathcal{T} : Y_i \in \hat{C}_{n_0, t}(X_i)\}.$$

These issues may be problematic when comparing the empirical performance of various methods—e.g., if we see one method has wider prediction intervals than another, is this a genuine difference or might it simply be due to overcoverage arising from rounding error or from ties? For this reason we use a modified version of the procedure for our real data experiments, as detailed next.

To alleviate this issue of overcoverage, Vovk et al. [27] proposes a randomization strategy, referred to as “smoothed conformal predictors” in that work. Here we show calculations for how to specialize Vovk et al. [27]’s randomization strategy to the specific setting of split conformal via nested sets, as constructed in (4).

Let $k = \lceil(1 - \alpha)(n_1 + 1)\rceil$, and let $\delta = k - (1 - \alpha)(n_1 + 1)$, capturing the rounding error. Let t_i be defined as above for each $i = n_0 + 1, \dots, n$ in the calibration set, and define the order statistics $t_{(1)} \leq \dots \leq t_{(n_1)}$ of this list. Define

$$T_0 = \#\{i \leq k - 1 : t_{(i)} = t_{(k-1)}\} \text{ and } T_1 = \#\{i \geq k : t_{(i)} = t_{(k)}\},$$

which capture information about the number of ties for $(k - 1)$ st or k th place. Then we

split into two cases: if $t_{(k-1)} < t_{(k)}$, then define

$$\hat{C}_n(X_{n+1}) = \begin{cases} (\hat{q}_{\text{lo}}(X_{n+1}, t_{(k-1)}), \hat{q}_{\text{hi}}(X_{n+1}, t_{(k-1)})), & \text{with probability } \frac{\delta}{T_0+1}, \\ [\hat{q}_{\text{lo}}(X_{n+1}, t_{(k-1)}), \hat{q}_{\text{hi}}(X_{n+1}, t_{(k-1)})], & \text{with probability } \frac{\delta T_0}{T_0+1}, \\ (\hat{q}_{\text{lo}}(X_{n+1}, t_{(k)}), \hat{q}_{\text{hi}}(X_{n+1}, t_{(k)})), & \text{with probability } \frac{(1-\delta)T_1}{T_1+1}, \\ [\hat{q}_{\text{lo}}(X_{n+1}, t_{(k)}), \hat{q}_{\text{hi}}(X_{n+1}, t_{(k)})], & \text{with probability } \frac{1-\delta}{T_1+1}, \end{cases}$$

while if instead $t_{(k-1)} = t_{(k)}$, then define

$$\hat{C}_n(X_{n+1}) = \begin{cases} (\hat{q}_{\text{lo}}(X_{n+1}, t_{(k)}), \hat{q}_{\text{hi}}(X_{n+1}, t_{(k)})), & \text{with probability } \frac{T_1+\delta}{T_0+T_1+1}, \\ [\hat{q}_{\text{lo}}(X_{n+1}, t_{(k)}), \hat{q}_{\text{hi}}(X_{n+1}, t_{(k)})], & \text{with probability } \frac{T_0+1-\delta}{T_0+T_1+1}. \end{cases}$$

Note that we might have $k = n_1 + 1$ (i.e., the order statistic $t_{(k)}$ is not defined, or rather, is taken to be $+\infty$). This happens in the case where $\alpha(n_1 + 1) < 1$. In this case, we take $t_{(n_1+1)} := +\infty$ and all the above definitions are still valid. (Observe that this scenario would fall into the first case, $t_{(k-1)} < t_{(k)}$, since $t_{(k-1)} = t_{(n_1)}$ is finite while $t_{(k)}$ is set to be $+\infty$.)

D Lipschitz property for UACQR-P

As mentioned earlier, the UACQR-P construction preserves the smoothness properties of the underlying base estimators. Here we will verify that if each of the bootstrapped estimates $\hat{q}_{Y|X}^b(x, a)$ is L -Lipschitz (as a function of x), then this property is preserved by the function $\hat{q}_{Y|X}^{(b)}(x, a)$, for each b . In particular, the left- and right-endpoint functions of the prediction band $\hat{C}_n = \{\hat{C}_n(x)\}$ will then be L -Lipschitz as well. The following basic result verifies this claim.

Proposition 1. *Let $f_1, \dots, f_B : \mathcal{X} \rightarrow \mathbb{R}$, where \mathcal{X} is a normed space. For any $b \in \{1, \dots, B\}$, define the function $f_{(b)} : \mathcal{X} \rightarrow \mathbb{R}$ as*

$$f_{(b)}(x) = \inf \left\{ t \in \mathbb{R} : \sum_{i=1}^B \mathbf{1}_{f_i(x) \leq t} \geq b \right\}.$$

(In other words, for each x , $f_{(1)}(x) \leq \dots \leq f_{(B)}(x)$ are the order statistics of $f_1(x), \dots, f_B(x)$. Then, if f_b is L -Lipschitz for all b , it holds that $f_{(b)}$ is L -Lipschitz for all b .

Proof. Suppose $f_{(b)}$ is not L -Lipschitz. Then there must exist some $x_0, x_1 \in \mathcal{X}$ with $|f_{(b)}(x_0) - f_{(b)}(x_1)| > L\|x_0 - x_1\|$. Without loss of generality, we can assume $f_{(b)}(x_1) > f_{(b)}(x_0)$.

By definition of $f_{(b)}(x_0)$ as the b th order statistic of $f_1(x_0), \dots, f_B(x_0)$, we have

$$\sum_{i=1}^B \mathbf{1}_{f_i(x_0) \leq f_{(b)}(x_0)} \geq b.$$

Similarly, by definition of $f_{(b)}(x_1)$ as the b th order statistic of $f_1(x_1), \dots, f_B(x_1)$, we have

$$\sum_{i=1}^B \mathbf{1}_{f_i(x_1) \geq f_{(b)}(x_1)} \geq B - b + 1.$$

Combining these two facts, we must have at least one $i \in \{1, \dots, B\}$ for which it holds that

$$f_i(x_0) \leq f_{(b)}(x_0) \text{ and } f_i(x_1) \geq f_{(b)}(x_1) > f_{(b)}(x_0) + L\|x_0 - x_1\|.$$

This is a contradiction, since f_i is L -Lipschitz. \square

E Additional Experiments

E.1 Simulation

In Figure 2 we saw that UACQR methods are able to maintain conditional coverage near $X = 0$, where epistemic uncertainty was high, without overcovering significantly when epistemic uncertainty was low, near $X = 1$. In Figure 4, we see that this adaptivity usually yields more precise intervals on average. Near $X = 0$, the UACQR methods provide wider intervals than the existing methods in order to achieve conditional coverage. This does not yield wider intervals on average everywhere else, though, with UACQR methods providing intervals as narrow as other methods when epistemic uncertainty is low. This further demonstrates the locally adaptive properties of our methods in this simulation setting.

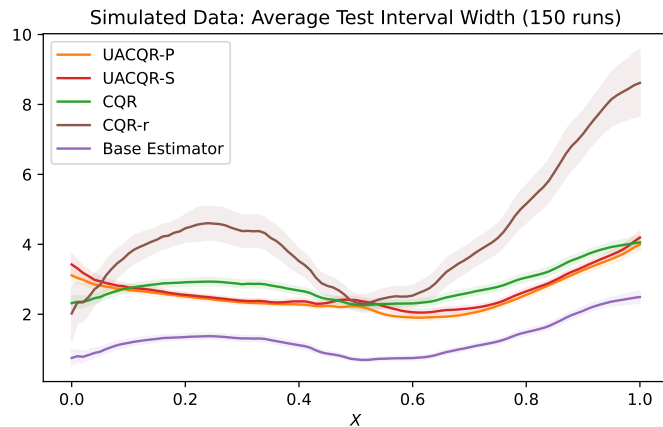


Figure 4: In the same setting as Figure 2, we see that the two UACQR methods have on average shorter interval widths than CQR and CQR-r for most values of X . When epistemic uncertainty is high ($X = 0$), our methods have wider intervals, allowing them to achieve conditional coverage in this region.

E.2 Real-world data sets

In this section, we test several alternative implementations of our real data experiments, to verify that our results persist across different choices made in the implementation.

In Table 2, we show results after taking a log transformation (specifically, replacing Y_i with $\log(1 + Y_i)$ for all data points, to allow for zero values). We do this instead of the usual mean normalization, so the units in Table 2 are different from other tables. All other details of the implementation remain the same. We observe that UACQR-P continues to show the best performance in terms of interval width on almost all data sets.

Table 2: Real data results on 20 runs with log transformation.

Dataset	Average Test Interval Width (Standard Error)			
	UACQR-P	UACQR-S	CQR	CQR-r
bike	1.613 (0.007)	1.901 (0.007)	1.946 (0.008)	1.886 (0.007)
bio	1.514 (0.006)	1.630 (0.004)	1.631 (0.004)	1.630 (0.004)
community	0.268 (0.003)	0.315 (0.003)	0.316 (0.002)	0.316 (0.002)
concrete	0.729 (0.010)	0.807 (0.008)	0.842 (0.007)	0.795 (0.008)
homes	0.596 (0.003)	0.635 (0.004)	0.650 (0.003)	0.634 (0.003)
star	0.175 (0.001)	0.174 (0.001)	0.174 (0.001)	0.174 (0.001)

In Table 3, we show the results after running the original experiment without the log transformation, except that we do not use randomization for handling ties/rounding (as detailed in Appendix C); instead, we use the original definition of the split nested conformal method given in (4) earlier. Here we see that the UACQR-P method is generally producing the shortest intervals, but CQR and CQR-r show a small improvement over UACQR-P for one data set (however, these improvements are comparable to the standard error of the results).

Table 3: Real data results on 20 runs with no randomized cutoffs.

Dataset	Average Test Interval Width (Standard Error)			
	UACQR-P	UACQR-S	CQR	CQR-r
bike	1.155 (0.009)	1.452 (0.008)	1.481 (0.008)	1.436 (0.008)
bio	1.548 (0.009)	1.650 (0.006)	1.652 (0.006)	1.649 (0.006)
community	1.527 (0.022)	1.752 (0.017)	1.762 (0.015)	1.759 (0.016)
concrete	0.691 (0.010)	0.734 (0.008)	0.750 (0.007)	0.727 (0.008)
homes	0.634 (0.004)	0.693 (0.005)	0.754 (0.005)	0.708 (0.005)
star	0.177 (0.001)	0.176 (0.001)	0.175 (0.001)	0.176 (0.001)

In Table 4, we show the results when the methods are run using a neural network, rather than Quantile Regression Forests, as the base algorithm. The model architecture is similar to what is described in Appendix B.1, except that we used an extensive hyperparameter

grid search over number of epochs, learning rate, batch size, weight decay penalty, dropout rate [26], and size of the hidden layers. For each method, we report the smallest average test interval width (across 20 trials) possible among 25 random draws of the hyperparameters. Again, we see that the UACQR-P method generally gives the shortest intervals.

Table 4: Real data results on 20 runs with neural network as base algorithm.

Dataset	Average Test Interval Width (Standard Error)			
	UACQR-P	UACQR-S	CQR	CQR-r
bike	0.854 (0.005)	1.011 (0.018)	1.037 (0.018)	0.997 (0.019)
bio	1.566 (0.005)	1.600 (0.008)	1.588 (0.006)	1.590 (0.007)
community	1.492 (0.023)	1.603 (0.025)	1.625 (0.030)	1.626 (0.027)
concrete	1.465 (0.009)	1.497 (0.011)	1.496 (0.010)	1.496 (0.010)
homes	0.552 (0.003)	0.602 (0.006)	0.602 (0.003)	0.603 (0.007)
star	0.179 (0.001)	0.187 (0.001)	0.187 (0.001)	0.189 (0.001)